

Optical microfiber phase modulator directly driven with low-power light

Zhangqi Song (宋章启)*, Yang Yu (于洋), Xueliang Zhang (张学亮),
Zhengtong Wei (卫正统), and Zhou Meng (孟洲)

College of Optoelectronic Science and Engineering, National University of Defense Technology,
Changsha 410073, China

*Corresponding author: songzhanqi@126.com

Received May 11, 2014; accepted July 16, 2014; posted online August 26, 2014

An optical microfiber phase modulator (OMPM) directly driven with low-power light is presented. Phase modulation response of OMPM is theoretically analyzed. A 10-mm optical microfiber (OM), tapered from conventional single-mode fiber, is inserted in one arm of a Michelson fiber interferometer. To drive the OMPM, 980-nm wavelength light with sinusoidal intensity modulation is injected into the interferometer. The OMPM response properties are measured and π -phase modulation amplitude can be obtained with only 7.5-mW average power light at 1-kHz modulation frequency. The OMPMs shown in this study have advantages of simple structure, potential compact size, and low-power-driven light.

OCIS codes: 060.2430, 120.5060, 250.4110.

DOI: 10.3788/COL201412.090606.

Optical microfibers (OMs) have attracted much attention due to their striking properties^[1,2]. A variety of tiny optical fiber components, including couplers^[3], filters^[4], Bragg gratings^[5], resonators^[6,7], mirrors^[8,9], phase modulators^[10], and interferometers^[11], have been shown using OMs. Optical phase modulator is one of important components in various optical systems. Now most of optical phase modulators, based on electro-optic effect, thermo-optic effect, or elastic-optic effect and driven with electrical signal^[12,13], are too big for compact OM interferometer. An OM phase modulator (OMPM) with megahertz bandwidth has been proposed. It is based on elastic-optic effect by stretching an OM wound on a piezoelectric ceramic rod with 1-mm diameter^[10]. But this OMPM needs hundreds of volts driving signal to get π -phase modulation. Heat generation within optical fiber is a phenomenon well known in fiber lasers and fiber amplifiers^[13, 14]. An optical-path-length modulator was shown with the thermo-optic effect^[15]. To produce enough optical-path-length change, it needs high-power pump laser and special doped optical fiber. And its phase shift responses slowly to the thermal modulation because of the big size of the standard optical fiber.

This letter presents an all-optical phase modulator that relies on direct heating of a short section of OM with a 980-nm pump laser. The OM is tapered from conventional single-mode fiber (SMF) specially by controlling the heating temperature of heater in the OM fabrication system^[9]. The transmitting loss in the OM is more than 10^5 times higher than that in a standard communication fiber. Then the heat generated in the OM is much more than a standard communication fiber with the same length. So we need not dope the OM to maximize the conversion of optical pump power into heat. The OM is easy to be heated up with low-power pump light because it has less volume and can confine light in a very small area over its waist region. In addition, the OM also has large surface-to-volume ratio, which allows the heat flowing out of its surface effectively.

All these make the OMPM to be an applicable phase modulator with high phase sensitivity and short response time. The OMPM can be driven by dislocated pump light, so it can be considered as an all-optical component and used in some specific places such as underwater or electromagnetic environment.

The phase modulation process in the OM with intensity-modulated 980-nm pump light is analyzed theoretically. We assume that the absorbing region of the OM is long and the loss of the OM is small, so that the longitudinal temperature gradient within waist region of the OM is small and longitudinal thermal conduction can be neglected. For the small size of the OM (usually several micrometers), radial temperature gradient is neglected here too. When a continuous sinusoidal modulated pump light with frequency f and amplitude P_0 , expressed as $P_0 \sin(2\pi ft)$, is launched into an OM at room temperature, the phase shift in the OM excited by the pump light can be obtained according to the heat conduction equation^[14]:

$$\Delta\Phi(t) = \frac{2\pi}{\lambda} \frac{\partial n}{\partial T} \frac{\eta BP_0 L \sin(2\pi ft - \theta)}{\sqrt{(2\pi f)^2 + A^2}} - \frac{2\pi}{\lambda} \frac{\partial n}{\partial T} \frac{ABP_0 L e^{-At}}{\sqrt{(2\pi f)^2 + A^2}}, \quad (1)$$

$$A = \frac{2h}{\rho c_v r}, \quad B = \frac{\alpha}{\pi r^2 \rho c_v},$$

where λ is the light wavelength in vacuum of the probe light; $\partial n/\partial T$ is refraction index temperature coefficient (here we omit the thermal expansion of the OM because its contribution is about 50 times smaller than that due to refraction index change); α is the local loss coefficient; L is the length of the OM; η is the fraction of the absorbed pump power that is turned into heat; h is the heat transfer coefficient of air that is related to the thermal conductivity k_a of air and the radius r of the OM waist region^[13]; ρ , c_v , and θ are the density, specific heat

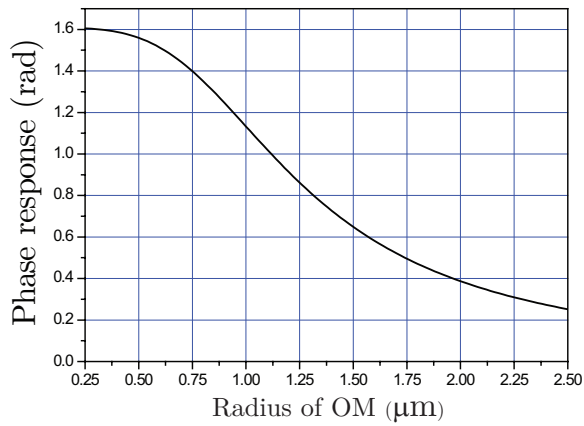


Fig. 1. Calculated phase responses of the OMPMs with different radii.

of the OM, and phase delay that is also contributed with the pump light power and the OM radius, respectively.

The second term in Eq. (1) is steady-state thermal response, which can be neglected as we impose continuous sinusoidal modulated pump light. The first term in Eq. (1) represents the sinusoidal phase response of the OMPM. We can get the phase response amplitude information at any frequency in the bandwidth.

According to the first term of Eq. (1), it can be found that the amplitude of phase response depends on the radius of the OM. To show the relationship between the amplitude of phase response and the OM radius, we simulated the phase response for the OMs with radii from 0.25 to 2.5 μm at the frequency 1 kHz. The results are shown in Fig. 1. The amplitude of phase response is about 1.1 rad when OM radius is 1 μm , which is high enough for phase modulation application. But its phase response decreases rapidly with the increasing OM radius. It has very limited phase response when radius is larger than 2.5 μm . Figure 1 was generated for silica OMs with $c_v = 741 \text{ J/kg/K}$, $r = 2.2 \times 10^3 \text{ kg/m}^3$. And h is calculated from Eq. (44) in Ref. [14] by using the thermal conductivity of air $k_a = 0.0254 \text{ W/m/K}$ at room temperature 20 $^\circ\text{C}$. The probe light wavelength is $\lambda = 1550 \text{ nm}$, and $\partial n/\partial T = 1.1 \times 10^{-5}/\text{K}$, $h = 20\%$, $\alpha = 0.05 \text{ dB/mm}$, $L = 10 \text{ mm}$, $P_0 = 10 \text{ mW}$. The OM in our experiment is taped from a section of normal communication optical fiber which has much higher extrinsic absorption at 980 nm than intrinsic absorption because of hydroxyls and dopants. And OM has even higher extrinsic absorption because water and contaminant in air are absorbed into OM and there are more impurities in OM tapered in common lab circumstance. So we assumed that 20% loss pump light turned into heat.

We have set up an interferometer system to measure the response of the OMPMs driven by the intensity-modulated light. The experimental configuration is shown in Fig. 2. For convenience, we choose 980-nm light as pump light and 1550-nm light as probe light.

The setup used an optical fiber coupler at 1550-nm and two Faraday rotator mirrors (FRMs) to form a Michelson interferometer. The probe light is a 1550-nm

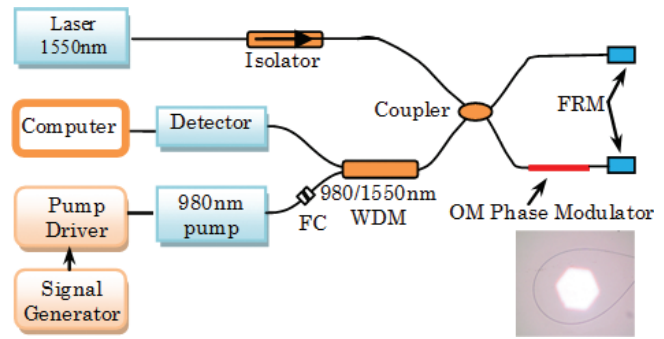


Fig. 2. Schematic diagram of the measurement system.

semiconductor laser source (linewidth 2-kHz; RIO). Light was continuously injected into the interferometer through an optical isolator. The 1550-nm output light of the interferometer was connected to a detector (model 1623, New Focus) through a 980/1550-nm wavelength division multiplexing (WDM). The WDM was used to couple 980-nm pump light into the OMPM in one arm of the interferometer and to filter any returned 980-nm light avoiding it going into the detector. The 980-nm pump laser was driven by a laser diode controller (LDC-37488B; ILX Lightwave), which could modulate the output light by connecting a sinusoidal electrical signal. An OM, 10-mm long with 0.5-dB loss and 1- μm radius, was inserted in one arm of the interferometer. It was measured that about 70% of 980-nm pump light was coupled into this arm.

Firstly, a sinusoidal modulation signal, with 1-kHz frequency and 160-mV amplitude, was imposed on the 980-nm pump driver. The output of the 980-nm pump laser was measured directly from the fiber connector (FC) placed with another photodetector and an oscilloscope. We adjusted the bias of the electrical modulation signal till the modulation depth of the output light was measured to be nearly 100%. Then, we connected the FC into the system shown in

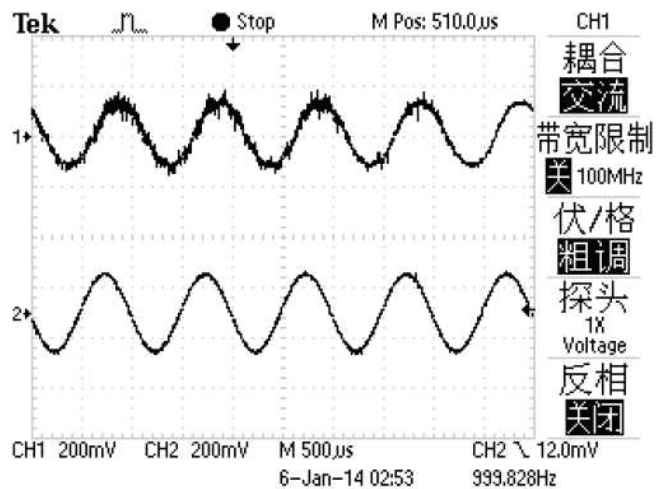


Fig. 3. Oscilloscope display of the output of the interferometer (top waveform) and the modulation signal (bottom waveform).

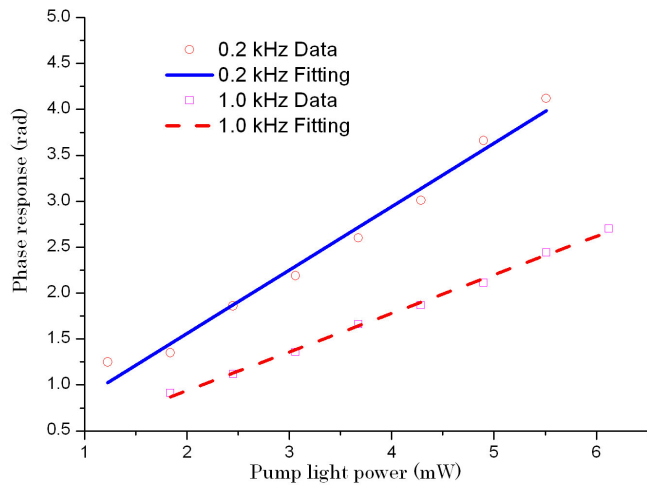


Fig. 4. Measured (dots) and fitted (line) linear responses of the OM (1- μm radius and 10-mm length) phase modulator with different average pump powers at 0.2- and 1-kHz frequencies.

Fig. 2 again. The output of the interferometer is measured with an oscilloscope, and the modulated signal was caught, as shown at the top of Fig. 3. The waveform (bottom) in Fig. 3 is the sinusoidal modulation electrical signal.

The phase shift of probe light caused by cross-phase modulation in OM is estimated. The nonlinear-index coefficient n_2 for fused silica is about $2.6 \times 10^{20} \text{ m}^2/\text{W}$. Assuming the power amplitude of 980-nm light launched into OM is 10 mW, the length of OM is 10 mm, the phase shifts of probe light caused by Kerr effect in OM with 1- μm radius and conventional fiber are about 6.7×10^6 and 2.7×10^5 rad, respectively. So the phase induced by Kerr effect in this letter can be omitted. The leakage of the 980-nm pump light is also considered. During the experiment, if we switched off the 1550-nm laser, the output waveform of the interferometer disappeared. It proves that the output waveform is from 1550-nm interference fringes, not from the intensity-modulated 980-nm pump light. We replaced the OM with a piece of conventional SMF, and then we could not observe the same phenomenon. The above processes have verified that the OM in the interferometer have worked as a phase modulator driven by the intensity-modulated 980-nm pump light, and it is an all-optical phase modulator.

To measure the amplitude responses of the OMPM, we sampled the output of the detector with an A/D converter (NI6251) and recorded it using a computer. Harmonics of the signal were used to calculate the amplitude of the phase modulation produced by the 980-nm light-modulating OMPM. By varying the amplitude of modulating signals imposed on the 980-nm laser driver at frequencies 1- and 0.2-kHz, a series of results were obtained (Fig. 4). As we can see, the results show that the OMPM has a good linearity with average power of driven light. The OMPM coefficients are 0.42 and 0.68 rad/mW at 1- and 0.2-kHz, respectively, which means we can get π -phase modulation amplitude with only 7.5-mW average power light at 1-kHz modulation frequency. This OMPM has higher phase response than

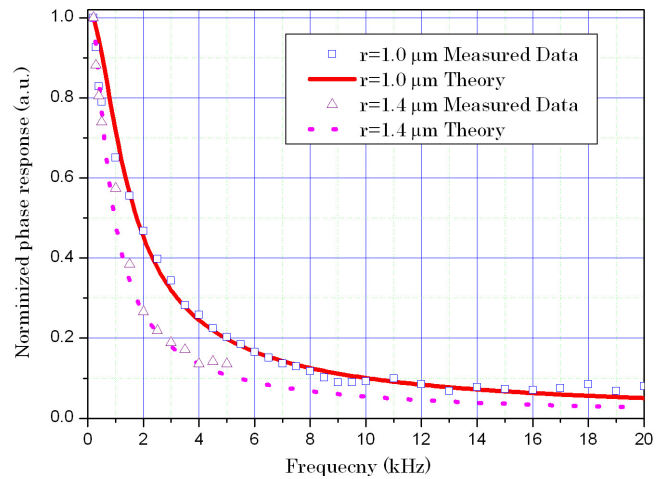


Fig. 5. Measured frequency response of two all-optical OMPMs (with OM radii 1 and 1.4 μm).

our simulation result, which may be due to the contribution of the OM conical parts, which is several times longer than the waist zone, or more fraction of the absorbed pump power is turned into heat. Further work is needed to explore this possibility.

We have made another OM sample 10-mm long with 1.4- μm radius, whose loss is also about 0.5 dB. The 1.4- μm OM has also been studied to act as a phase modulator. Adjusting the modulating frequency with the 980-nm driving light intensity keeping constant, the frequency responses of 1- and 1.4- μm OMPMs were also measured in the system. The average optical power of the intensity-modulated 980-nm pump light imposed on the OMPM was measured to be 5.6 mW. To eliminate the effects of the length and local loss of the OM, we normalized the values of the measured frequency responses with the phase modulation amplitude at frequency 0.2 kHz. The measured data and theoretical frequency response curves are normalized and plotted in Fig. 5.

It is evident that the measured frequency responses are well consistent with the theoretical analysis. The modulation signal has been measured up to 20 kHz with 1- μm OMPM. The frequency response of the OMPM with 1.4- μm radius has been measured only up to 5 kHz because the modulation signal has become so small that it is difficult to calculate phase shift with the harmonics method. The response times of 1- and 1.4- μm radii are 0.16 and 0.31 ms, respectively. The response times of 1- and 1.4- μm radii are 0.16 and 0.31 ms, respectively.

In conclusion, we propose and show OMPMs based on OMs tapered from conventional SMF. The phase modulation is obtained by directly heating the OM with 980-nm light, which is intensity modulated. The OMPM can reach frequency responses in excess of 20 kHz with 1- μm radius driven by 5.6-mW 980-nm modulated light. This kind of device is potentially valuable in evaluation of tiny all-optical interferometers and could find use in fiber optics system, such as the underwater and electromagnetic environment, for the intensity-modulated light is remotely adopted.

References

1. L. Tong, F. Zi, X. Guo, and J. Lou, *Opt. Commun.* **285**, 4641 (2012).
2. G. Brambilla, *J. Opt.* **12**, 043001 (2010).
3. A. Sulaiman, S. W. Harun, and H. Ahmad, *Chin. Opt. Lett.* **12**, 021403 (2014).
4. X. Jiang, Y. Chen, G. Vienne, and L. Tong, *Opt. Lett.* **32**, 1710 (2007).
5. M. Ding, M. N. Zervas, and G. Brambilla, *Opt. Express* **19**, 15621 (2011).
6. Z. Chen, V. K. Hsiao, X. Li, Z. Li, J. Yu, and J. Zhang, *Opt. Express* **19**, 14217 (2011).
7. M. Sumetsky, A. Y. Dulashko, J. M. Fini, and A. Hale, *Appl. Phys. Lett.* **86**, 161108 (2005).
8. S. Wang, Z. Hu, Y. Li, and L. Tong, *Opt. Lett.* **34**, 253 (2009).
9. Y. Yu, X. Zhang, Z. Song, Z. Wei, and Z. Meng, *Chin. Opt. Lett.* **12**, 012301 (2014).
10. X. Zhang, M. Belal, G. Y. Chen, Z. Song, G. Brambilla, and T. P. Newson, *Opt. Lett.* **37**, 320 (2012).
11. Y. Li and L. Tong, *Opt. Lett.* **33**, 303 (2008).
12. S. A. Clarka, B. Cuishawa, E. J. C. Dawnayb, and I. E. Days, *Proc. SPIE* **3936**, 16 (2000).
13. E. L. Wooten, K. M. Kissa, A. Yi-Yan, E. J. Murphy, D. A. Lafaw, P. F. Hallemeier, D. Maack, D. V. Attanasio, D. J. Fritz, G. J. McBrien, and D. E. Bossi, *IEEE J. Sel. Top. Quant.* **6**, 69 (2000).
14. M. K. Davis, M. J. F. Digonnet, and R. H. Pantell, *J. Lightwave Technol.* **16**, 1013 (1998).
15. Z. Matjasec, S. Campelj, and D. Donlagic, *Opt. Express* **21**, 11794 (2013).